Cell Death and Differentiation (2009) 16, 1040–1052

www.nature.com/cdd

Superoxide is the major reactive oxygen species regulating autophagy

Y Chen[1,2], MB Azad[1,2] and SB Gibson*[,1,2]

Autophagy is involved in human diseases and is regulated by reactive oxygen species (ROS) including superoxide ($O_2^{\bullet -}$) and hydrogen peroxide (H_2O_2). However, the relative functions of $O_2^{\bullet -}$ and H_2O_2 in regulating autophagy are unknown. In this study, autophagy was induced by starvation, mitochondrial electron transport inhibitors, and exogenous H_2O_2. We found that $O_2^{\bullet -}$ was selectively induced by starvation of glucose, L-glutamine, pyruvate, and serum (GP) whereas starvation of amino acids and serum (AA) induced $O_2^{\bullet -}$ and H_2O_2. Both types of starvation induced autophagy and autophagy was inhibited by overexpression of SOD2 (manganese superoxide dismutase, Mn-SOD), which reduced $O_2^{\bullet -}$ levels but increased H_2O_2 levels. Starvation-induced autophagy was also inhibited by the addition of catalase, which reduced both $O_2^{\bullet -}$ and H_2O_2 levels. Starvation of GP or AA also induced cell death that was increased following treatment with autophagy inhibitors 3-methyladenine, and wortamannin. Mitochondrial electron transport chain (mETC) inhibitors in combination with the SOD inhibitor 2-methoxyestradiol (2-ME) increased $O_2^{\bullet -}$ levels, lowered H_2O_2 levels, and increased autophagy. In contrast to starvation, cell death induced by mETC inhibitors was increased by 2-ME. Finally, adding exogenous H_2O_2 induced autophagy and increased intracellular $O_2^{\bullet -}$ but failed to increase intracellular H_2O_2. Taken together, these findings indicate that $O_2^{\bullet -}$ is the major ROS-regulating autophagy.
Cell Death and Differentiation (2009) **16,** 1040–1052; doi:10.1038/cdd.2009.49; published online 1 May 2009

Autophagy is a lysosomal degradation process characterized by the formation of double-membraned autophagosomes. During autophagy, cytoplasmic material and organelles are sequestered by an isolation membrane derived from the preautophagosomal structure. Fusion of this double-membraned vesicle creates an autophagosome, which ultimately fuses with a lysosome. Within the resulting autophagolysosome, the sequestered cytoplasmic materials are degraded by acidic hydrolases. Autophagic degradation generates amino acids and fatty acids that can be used for protein synthesis or oxidized through the mitochondrial electron transport chain (mETC) to produce ATP for cell survival under starvation conditions.[1] However when autophagy is prolonged, proteins and organelles essential for basic homeostasis and cell survival are degraded, which can lead to cell death (autophagic cell death or programmed cell death type II, PCD II).[2] Therefore, autophagy is both a cell survival mechanism and a cell death pathway depending on the extent of cellular degradation.

Reactive oxygen species (ROS) are molecules or ions that are formed by the incomplete one-electron reduction of oxygen. The major species of ROS include superoxide ($O_2^{\bullet -}$), hydrogen peroxide (H_2O_2), and hydroxyl radical ($^{\bullet}OH$).[3] These three major ROS are mainly produced through a chain reaction as follows: $O_2^{\bullet -}$, which is mainly produced from mETC complexes I and III, is converted to H_2O_2 by the superoxide dismutase (SOD) family of enzymes, which mainly include SOD1 (copper-zinc superoxide dismutase, Cu, Zn-SOD) and SOD2 (manganese superoxide dismutase, Mn-SOD). H_2O_2 can then be converted to $^{\bullet}OH$ by ferrous iron (Fe^{2+}) or copper ion (Cu^{+}), or it can be catalyzed to H_2O by catalase, glutathione peroxidase (GPx) and peroxiredoxin III (PrxIII).[3] Thus, the levels of $O_2^{\bullet -}$, H_2O_2, and $^{\bullet}OH$ are constantly in flux until an equilibrium is established.

It is well known that ROS can regulate apoptosis (PCD type I).[4] ROS regulation of autophagy has also been demonstrated in many reports.[5–22] Most of these studies have implicated ROS in autophagy induction by using nonspecific ROS scavengers or exogenous H_2O_2.[5,7-9,12,14,21] Our previous studies suggest that $O_2^{\bullet -}$ specifically mediates autophagy induced by mETC inhibitors (complex I inhibitor rotenone and complex II inhibitor 2-thenoyltrifluoroacetone (TTFA)), the SOD inhibitor 2-methoxyestradiol (2-ME),[23] and exogenous H_2O_2.[3,17,18] Kim *et al.*[13] have demonstrated that sodium-selenite-induced autophagy is also regulated by $O_2^{\bullet -}$. In contrast, several reports have specifically implicated H_2O_2 in regulating autophagy.[11,16,19,20,22] Thus, it seems that both $O_2^{\bullet -}$ and H_2O_2 are involved, however none of the previous

[1]Manitoba Institute of Cell Biology, University of Manitoba, Winnipeg, Manitoba, Canada and [2]Department of Biochemistry and Medical Genetics, Faculty of Medicine, University of Manitoba, Winnipeg, Manitoba, Canada
*Corresponding author: SB Gibson, Manitoba Institute of Cell Biology, University of Manitoba, 675 McDermot Ave, Winnipeg, Manitoba R3E 0V9, Canada.
Tel: +204 787 2051; Fax: +204 787 2190; E-mail: gibsonsb@cc.umanitoba.ca
Keywords: autophagy; superoxide; superoxide dismutase; reactive oxygen species; starvation; mitochondrial electron transport chain
Abbreviations: AA, amino acids and serum; AO, acridine orange; AVOs, acidic vesicular organelles; CM-H2DCFDA, 5-(and-6)-chloromethyl-2′,7′-dichlorodihydrofluorescein diacetate acetyl ester; DHE, dihydroethidium; 2-ME, 2-methoxyestradiol; 3-MA, 3-methyladenine; GFP, green fluorescent protein; GP, glucose, L-glutamine, pyruvate and serum; GPx, glutathione peroxidase; H_2O_2, hydrogen peroxide; LC3, microtubule-associated protein 1 light chain 3; mETC, mitochondrial electron transport chain; NAC, *N*-acetyl-cysteine; $O_2^{\bullet -}$, superoxide; $^{\bullet}OH$, hydroxyl radical; PCD, programmed cell death; PrxIII, peroxiredoxin III; ROS, reactive oxygen species; SOD, superoxide dismutase; SOD1, copper-zinc superoxide dismutase (Cu, Zn-SOD); SOD2, manganese superoxide dismutase (Mn-SOD); TTFA, 2-thenoyltrifluoroacetone
Received 31.10.08; revised 23.3.09; accepted 25.3.09; Edited by D Klionsky; published online 01.5.09

studies has investigated the relative functions of both species in the regulation of autophagy. Thus, the ROS responsible for regulating autophagy remains unclear.

In this study we have investigated the relative functions of $O_2^{\bullet -}$ and H_2O_2 in autophagy induced by starvation, mETC inhibitors, and exogenous H_2O_2. We found that the levels of autophagy induced by starvation, mETC inhibition, and exogenous H_2O_2 correlated with increased $O_2^{\bullet -}$ levels and decreased H_2O_2 levels. Furthermore, starvation-induced cell death was increased by the inhibition of autophagy with autophagy inhibitors and $O_2^{\bullet -}$ scavengers but decreased by the enhancement of autophagy by knocking down SOD2 expression. In contrast, cell death induced by mETC inhibitors was elevated by the enhancement of autophagy with SOD2 inhibition. These results give significant insights into the regulation of autophagy.

Results

Starvation induces ROS generation. Several reports have suggested that starvation-induced autophagy is mediated by ROS.[5–22] In this study, we investigated the generation of $O_2^{\bullet -}$ and H_2O_2 under two starvation conditions: starvation of glucose, L-glutamine, pyruvate, and serum (GP), and starvation of amino acids and serum (AA). Cellular levels of $O_2^{\bullet -}$ and H_2O_2 were measured by flow cytometry using specific fluorescent dyes (see Materials and Methods). Figure 1 shows that over a 72-h time course in HeLa cells, GP or AA starvation increased $O_2^{\bullet -}$ levels to 50% compared with 10% in control conditions (also Supplementary Figure S1). GP starvation did not induce H_2O_2 generation (Figure 1a) whereas AA starvation induced H_2O_2 generation up to 80% (Figure 1b; Supplementary Figure S1). Generation of $O_2^{\bullet -}$ and H_2O_2 was not significant before 6 h of starvation. Similar results were also obtained in U87 cells (Supplementary Figure S2) and HEK293 cells (data not shown). Thus, both GP and AA starvation increased $O_2^{\bullet -}$ levels but only AA starvation increased H_2O_2 levels.

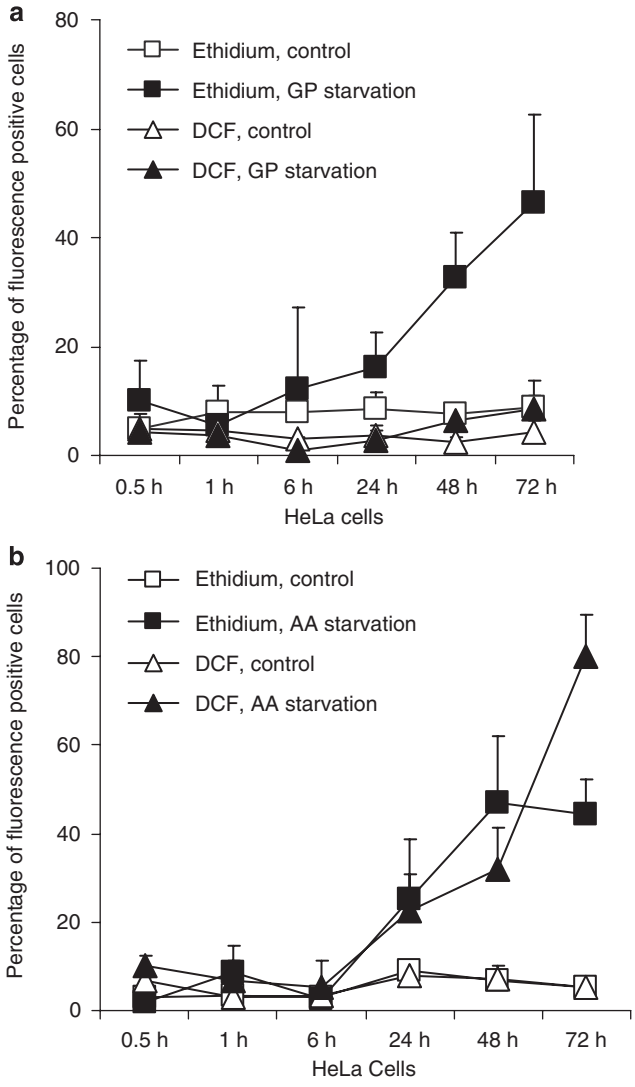

Figure 1 Starvation induces ROS generation in HeLa cells over a 72-h time course. (**a**) Starvation of GP (glucose, L-glutamine, pyruvate, and serum). (**b**) Starvation of AA (amino acids and serum). Intracellular $O_2^{\bullet -}$ and H_2O_2 were measured by flow cytometry after cells were stained with DHE (dihydroethidium) and CM-H2DCFDA (5-(and-6)-chloromethyl-2′,7′-dichlorodihydrofluorescein diacetate acetyl ester), respectively, as stated in Materials and Methods section. Because DHE is oxidized to ethidium by $O_2^{\bullet -}$ and CM-H2DCFDA is oxidized to DCF (dichlorofluorescein) by H_2O_2, the percentages of ethidium fluorescence and DCF fluorescence represent the levels of intracellular $O_2^{\bullet -}$ and H_2O_2, respectively. Error bars represent standard deviation (S.D.) from three independent duplicate experiments

Starvation induces autophagy. It is well known that starvation can induce autophagy.[1] In this study, we detected starvation-induced autophagy using three methods as in our previous studies.[17,18,24] We transiently transfected cells with GFP-LC3, which is recruited to autophagosome membranes during autophagy resulting in a punctate distribution that can be visualized using a fluorescent microscope. We measured the formation of acidic vesicular organelles (AVOs, which include autolysosomes) by flow cytometry using the pH-sensitive fluorescent dye acridine orange (AO). Finally, we used western blotting to detect the conversion of cytosolic LC3-I to lipidated, autophagosome-membrane-bound LC3-II. Because LC3-II is continually degraded within autophagolysosomes during autophagy, it is recommended that cells be treated with a lysosomal inhibitor before western blotting for LC3-II to demonstrate autophagic flux.[25,26] In the presence of the lysosomal inhibitor NH_4Cl, GP or AA starvation in HeLa cells induced elevated levels of LC3-II at 24 and 48 h but not at 1 and 6 h (Figure 2a), correlating with ROS generation (Figure 1). Similar phenomena were also observed in U87 cells (Supplementary Figure S3). Starvation of GP or AA also induced the formation of GFP-LC3 puncta (Figure 2b) and AVOs (Figure 2c) in HeLa cells. Elevated amount of starvation-induced LC3-II and microtubule-associated protein 1 light chain 3 (LC3) puncta could be observed as early as at 24 h (Figure 2a and b) whereas elevated amount of starvation-induced AVOs could only be seen after 48 h (Figure 2c). This supports the current hypothesis that the formation of autolysosomes (which belong to AVOs) lags behind the formation of autophagosomes.[1] In the presence of 3-methyladenine (3-MA, a chemical inhibitor of

autophagy), starvation-induced LC3-II formation was significantly reduced (Figure 2d). 3-MA treatment also decreased starvation-induced formation of GFP-LC3 puncta and AVOs in HeLa cells: the percentage of GP or AA starved cells with GFP-LC3 puncta was reduced from 40 to 14%, whereas the percentage of cells with AVOs decreased from 33 to 2% (GP starvation), and from 18 to 2% (AA starvation) (Supplementary Figure S4a). Wortmannin, another autophagy inhibitor, decreased the percentage of cells with AVOs from 45 to 11% with GP starvation and from 37 to 6% with AA starvation (Supplementary Figure S4bi). Furthermore, when the autophagy genes *beclin-1* and *atg-7* were knocked down by siRNA in HeLa cells (Figure 2ei), starvation-induced LC3-II formation was reduced (Figure 2eii), and the percentage of cells with AVOs was reduced from 30 to 9% with GP starvation and from 23 to 2% with AA starvation (Supplementary Figure S4c). GFP-LC3 puncta was also reduced from 40 to 15% with GP starvation and from 34 to 13% with AA starvation (Supplementary Figure S4c). Therefore, both GP and AA starvation conditions induce autophagy to similar extents.

Under starvation conditions, autophagy is normally considered to be a cell survival mechanism.[1] To test this hypothesis, we investigated the effect of autophagy inhibition on

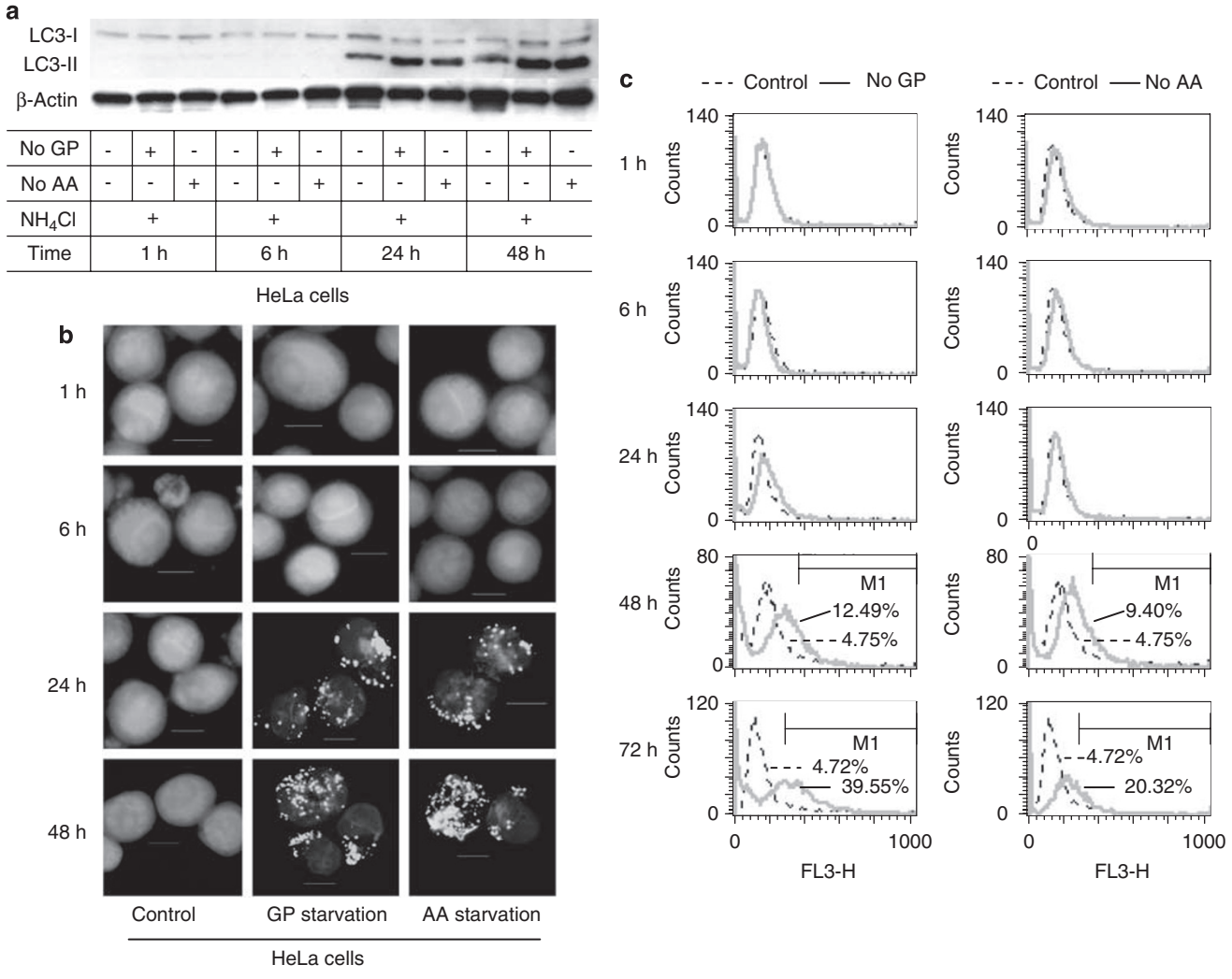

Figure 2 Starvation induces autophagy and cell death in HeLa cells. (**a**) Formation of LC3-II after cells were starved of GP or AA for 1, 6, 24, and 48 h. (**b**) Representative fluorescent microscopic figures of the formation of GFP-LC3 dots (puncta) after cells were transfected with GFP-LC3 cDNA and starved of GP or AA for 1, 6, 24, and 48 h. GFP-LC3 dots were not observed when cells were transfected with GFP cDNA (data not shown). Scale bars = 10 μm. (**c**) Representative histographs of AVOs formation analyzed by flow cytometry after cells were starved of GP or AA for 1, 6, 24, 48, and 72 h. The gated region (M1) in each histogram represents the percentage of cells with AVOs. (**d**) Effect of autophagy inhibitor 3-MA (2 mM) on formation of LC3-II after cells were starved of GP or AA for 48 h. (**e**) Effect of *beclin-1* and *atg-7* siRNAs on formation of LC3-II after cells were starved of GP or AA for 48 h. (i) Expression of beclin-1 and ATG-7 after cells were transfected with control, *beclin-1* and *atg-7* siRNAs. (ii) Western blot showing formation of LC3-II with β-actin used as a loading control. Cells were treated with the lysosomal inhibitor NH_4Cl at 30 mM for the determination of autophagy flux. (**f**) Cell death induced by GP or AA starvation. Cell death was analyzed by measuring the plasma membrane permeability by flow cytometry using Trypan blue to stain cells as described in Materials and methods section. The percentage of plasma membrane permeability represents the percentage of cell death. (i) Cell death induced by GP and AA starvation in a 72-h time course. (ii) Effect of 3-MA (2 mM) on GP or AA starvation-induced cell death at 24, 48, and 72 h. (iii) Effect of *beclin-1* and *atg-7* siRNAs on GP or AA starvation-induced cell death at 72 h. All data are representative of three independent experiments

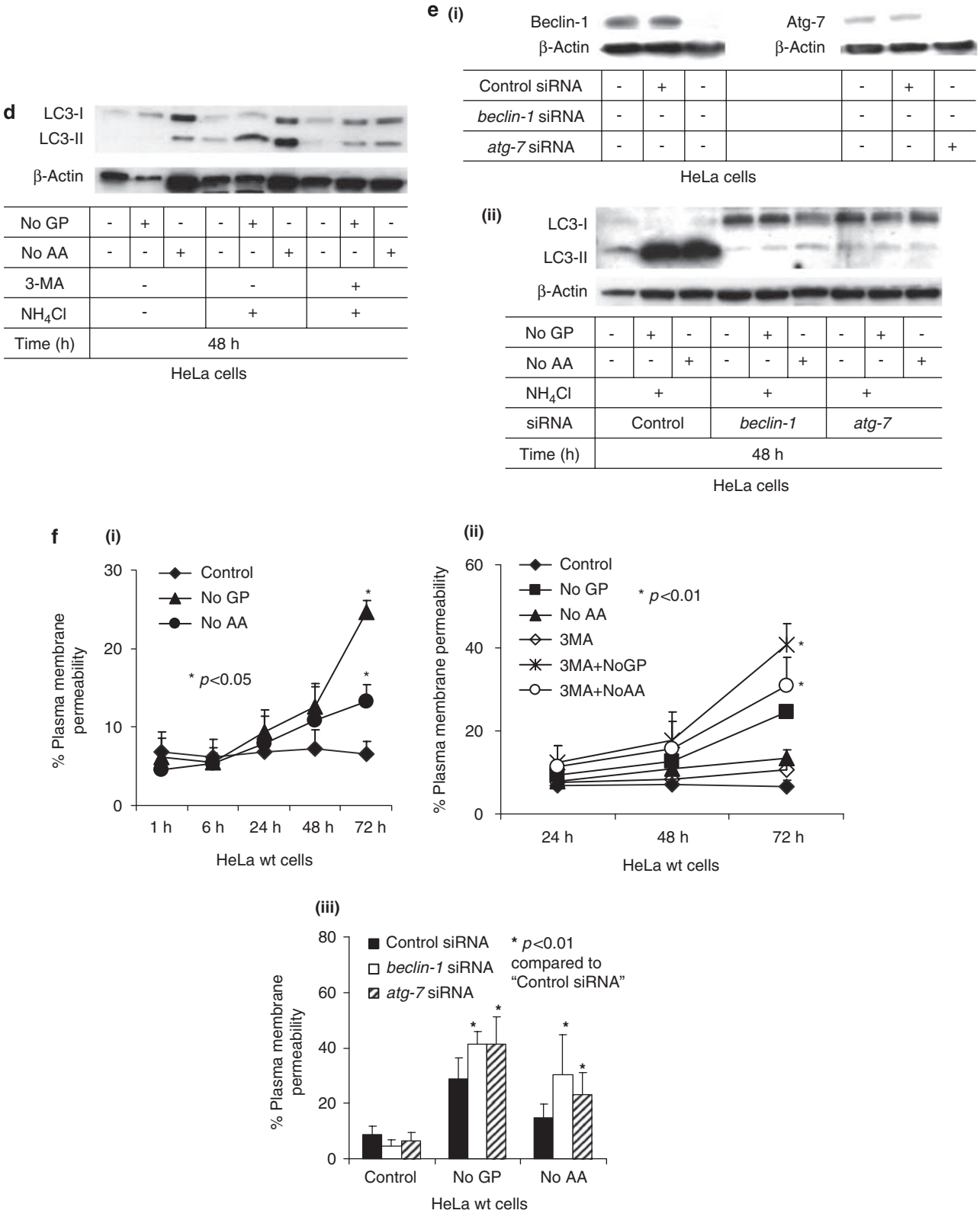

Figure 2 Continued

starvation-induced cell death in HeLa cells. Figure 2fi shows that GP starvation induced cell death up to 25% and AA starvation induced cell death only to 13% compared to 7% of cell death with non-starvation treatment after 72 h. When autophagy inhibitor 3-MA was added, GP starvation-induced cell death was elevated to 40% and AA starvation-induced cell

death was elevated to 30% (Figure 2fii). When another autophagy inhibitor wortmannin was added in HeLa cells, GP starvation-induced cell death was increased to 36% and AA starvation-induced cell death was increased to 43% (Supplementary Figure S4bii). GP or AA starvation-induced cell death was also significantly enhanced at 24 and 48 h (Supplementary Figure S4bii). When the autophagy genes *beclin-1* and *atg-7* were knocked down by siRNA in HeLa cells (Figure 2ei), GP starvation-induced cell death was increased from 29 to 41% and 41%, respectively, and AA starvation-induced cell death was increased from 15 to 30% and 23%, respectively (Figure 2fiii). This suggests that autophagy is a cell survival mechanism under GP and AA starvation conditions similar to other published results.[1]

Starvation-induced autophagy is mediated by $O_2^{\bullet -}$. Because both GP and AA starvation induced autophagy and $O_2^{\bullet -}$ production, and as H_2O_2 production was absent during GP starvation (Figure 1; Supplementary S1, and S2), we hypothesized that starvation-induced autophagy is specifically mediated by $O_2^{\bullet -}$. The production of $O_2^{\bullet -}$ and H_2O_2 is a chain reaction, where $O_2^{\bullet -}$ is converted to H_2O_2 by SOD, and H_2O_2 can either be converted to H_2O by other antioxidant enzymes (such as catalase, GPx, and PrxIII), or to $^{\bullet}OH$ by Fe^{2+} or Cu^{+}.[3] Therefore, the levels of $O_2^{\bullet -}$ and H_2O_2 can be adjusted by altering the antioxidant enzymes mentioned above. To determine the relative functions of $O_2^{\bullet -}$ and H_2O_2 in the regulation of starvation-induced autophagy, we manipulated the cellular levels of these two ROS species by modifying the level of SOD2 through overexpression and siRNA knockdown or by treating cells with exogenous catalase. In Figure 3, ROS generation and autophagy was determined in wild-type (wt) HeLa cells or HeLa cells with stable overexpression of SOD2 (SOD2) in the mitochondria (Figure 3a; Supplementary Figure S5). Because SOD2 catalyzes the conversion of $O_2^{\bullet -}$ to H_2O_2, we expected SOD2 cells to exhibit decreased $O_2^{\bullet -}$ levels and increased H_2O_2 levels. Compared to levels in the wt cells, both GP starvation-induced autophagy and $O_2^{\bullet -}$ levels in SOD2 cells were significantly decreased. In addition, the percentage of cells with AVOs and GFP-LC3 puncta decreased from 22 to 1% and from 32 to 13%, respectively, whereas $O_2^{\bullet -}$ generation was reduced from 30 to 8% in SOD2 cells (Figure 3b). As expected, GP starvation-induced H_2O_2 generation was significantly increased by SOD2 overexpression, from 7 to 20% (Figure 3b). Similarly, AA starvation-induced autophagy and $O_2^{\bullet -}$ generation were significantly decreased in SOD2 cells compared with that in wt cells. The percentage of cells with AVOs and GFP-LC3 puncta decreased significantly from 18 to 1% and from 38 to 13%, respectively, whereas $O_2^{\bullet -}$ generation was decreased from 33 to 4% in SOD2 cells (Figure 3c). AA starvation-induced H_2O_2 levels were 32% in both wt and SOD2 cells (Figure 3c). GP and AA starvation-induced LC3-II protein levels were also decreased in SOD2 cells compared to that in wt cells (Figure 3d). Because the inhibition of autophagy by 3-MA, wortmannin, and siRNAs against *beclin-1* and *atg-7* increased GP and AA starvation-induced cell death (Figures 2f; Supplementary Figure S4bii), it is expected that SOD2 overexpression would also elevate GP and AA starvation-induced cell death. This is demonstrated in Figure 3e. In the wt HeLa cells, starvation of GP or AA did not significantly increase cell death compared to control whereas in SOD2 HeLa cells, GP starvation increased cell death from 13 to 45%. Similarly, AA starvation increased cell death from 11 to 29% compared to that in wt cells at 48 h. After 72 h, SOD2 overexpression in cells increased GP starvation-induced cell death from 25 to 62% and increased AA starvation-induced cell death from 13 to 50% (Figure 3e). When autophagy inhibitors 3-MA (Figure 3f) and wortmannin (Supplementary Figure S4biii) were added, cell death induced by GP or AA starvation in SOD2 HeLa cells was not significantly affected. This indicates that when GP and AA starvation-induced autophagy was reduced to a very low level by $O_2^{\bullet -}$ scavenger SOD2 (Figure 3b, c, and d), addition of other autophagy inhibitors (3-MA, wortmannin) would not further increase the levels of cell death induced by GP or AA starvation.

Next, we used siRNA to knock down the expression of SOD2 in HeLa cells (Figure 4a). SOD2 knockdown increased starvation-induced $O_2^{\bullet -}$ levels from 60 to 80% (GP starvation) and from 40 to 74% (AA starvation) compared to cells transfected with control siRNA (Figure 4b). In addition, SOD2 knockdown significantly decreased AA starvation-induced H_2O_2 levels from 24 to 12% whereas GP starvation-induced H_2O_2 was not affected (Figure 4b), because no significant induction was observed (Figures 1a and 4b). Along with increased $O_2^{\bullet -}$ levels, SOD2 knockdown cells had higher levels of GP and AA starvation-induced autophagy: the percentage of cells with AVOs was increased from 31 to 50% and from 23 to 38%, respectively, whereas the percentage of cells with GFP-LC3 puncta was increased from 40 to 54% and from 34 to 55%, respectively (Figure 4b). LC3-II protein levels following GP and AA starvation were also significantly increased by SOD2 knockdown (Figure 4c). Thus, SOD2 knockdown cells had increased $O_2^{\bullet -}$ (with decreased or unchanged H_2O_2), and increased starvation-induced autophagy. In contrast to SOD2 overexpression (Figure 3e), SOD2 knockdown decreased GP starvation-induced cell death from 29 to 16% and AA starvation-induced cell death from 15 to 7% at 72 h (Figure 4d). This indicates that when starvation-induced autophagy is enhanced by SOD2 knockdown, starvation-induced cell death would be reduced, agreeing with the cell survival mechanism of autophagy under starvation conditions. Taken together, these data show that $O_2^{\bullet -}$ levels regulated by SOD2 are strongly correlated with starvation-induced autophagy.

Others have shown that exogenous catalase enzyme can be added to cells extracellularly to scavenge intracellularly produced H_2O_2.[8,15,22,27] Because cellular H_2O_2 is generated by a chain reaction from $O_2^{\bullet -}$, catalase can also indirectly reduce cellular $O_2^{\bullet -}$ levels.[3] The three major cellular ROS species, $O_2^{\bullet -}$, H_2O_2, and $^{\bullet}OH$, are in flux through a chain reaction.[2,3] $O_2^{\bullet -}$ that is mainly produced from mETC complexes I and III will be catalyzed to H_2O_2 by SOD. Then H_2O_2 can either be converted to $^{\bullet}OH$ by Fe^{2+} or Cu^{+} or be catalyzed to H_2O by catalase, GPx, and PrxIII. Therefore, we treated HeLa cells with catalase and compared autophagy, ROS induction, and cell death under control and starvation conditions (Figure 5). We found that starvation-induced $O_2^{\bullet -}$ was reduced from 52 to 5% (GP starvation) or from 54 to 10%

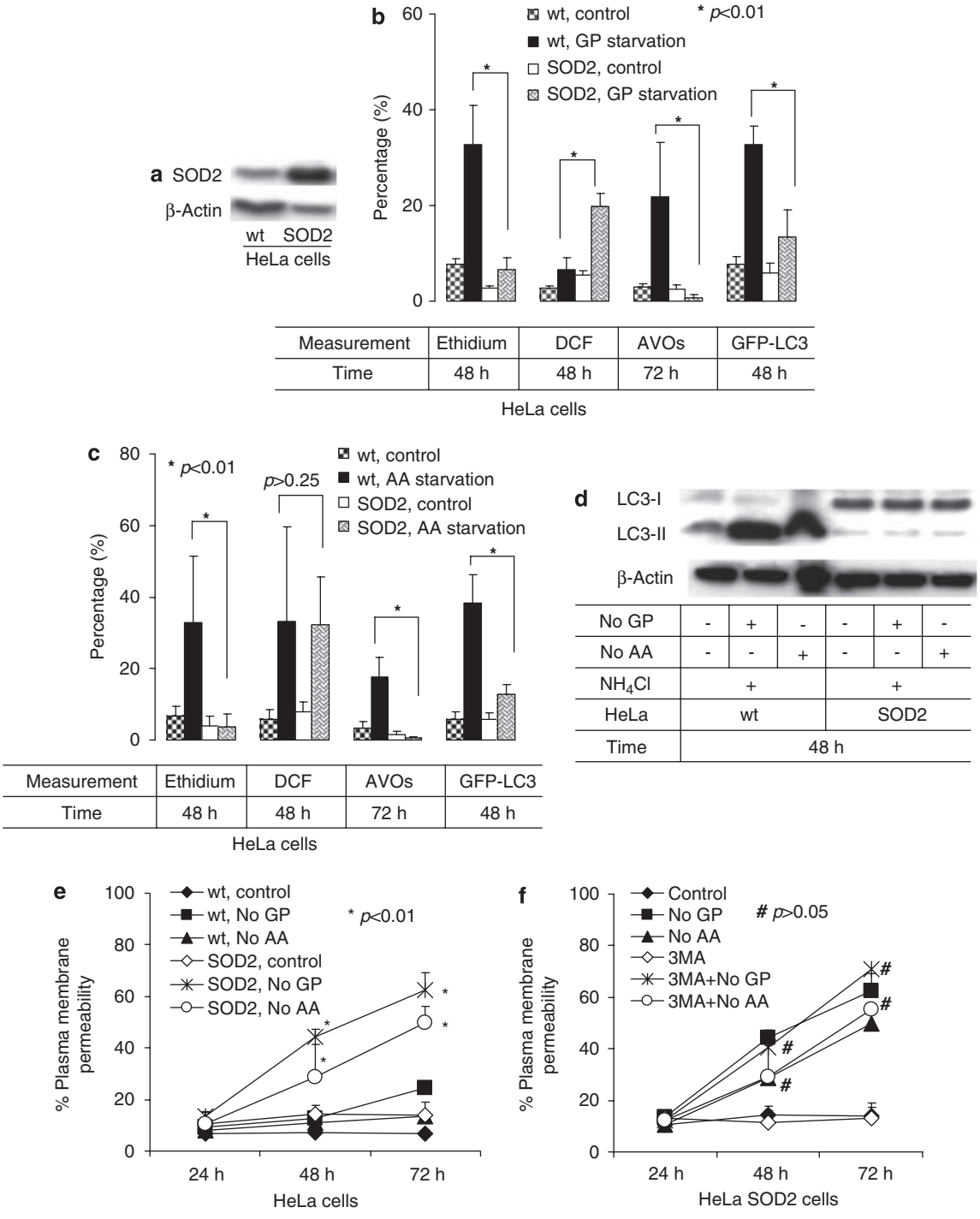

Figure 3 Overexpression of SOD2 downregulates autophagy but upregulates cell death induced by GP or AA starvation in HeLa cells. (**a**) Comparison of SOD2 expression between the wild-type (wt) and SOD2 overexpressing (SOD2) HeLa cells. β-Actin was used as a loading control. (**b** and **c**) Effect of SOD2 overexpression on ROS generation, formation of AVOs, and GFP-LC3 dots (puncta) induced by GP and AA starvation, respectively. The percentages of ethidium fluorescence and DCF fluorescence represent the levels of intracellular $O_2^{\bullet -}$ and H_2O_2, respectively, as described in Figure 1. (**d**) Effect of SOD2 overexpression on formation of LC3-II after cells were starved of GP or AA for 48 h. β-Actin was used as a loading control. Cells were treated with the lysosomal inhibitor NH_4Cl at 30 mM for the determination of autophagy flux. (**e**) Effect of SOD2 overexpression on GP or AA starvation-induced cell death at 24, 48, and 72 h. (**f**) Effect of 3-MA (2 mM) on GP or AA starvation-induced cell death in SOD2 overexpression cells at 24, 48, and 72 h. The percentage of plasma membrane permeability represents the percentage of cell death as described in Figure 2. Error bars represent standard deviation (S.D.). All data are representative of three independent experiments

(AA starvation), whereas H_2O_2 was reduced from 43 to 9% (AA starvation) after catalase treatment (Figure 5a). Although GP starvation did not significantly induce H_2O_2 production compared to control, the background level of H_2O_2 was reduced by catalase (Figure 5a). In addition to decreased ROS levels, catalase-treated cells exhibited decreased

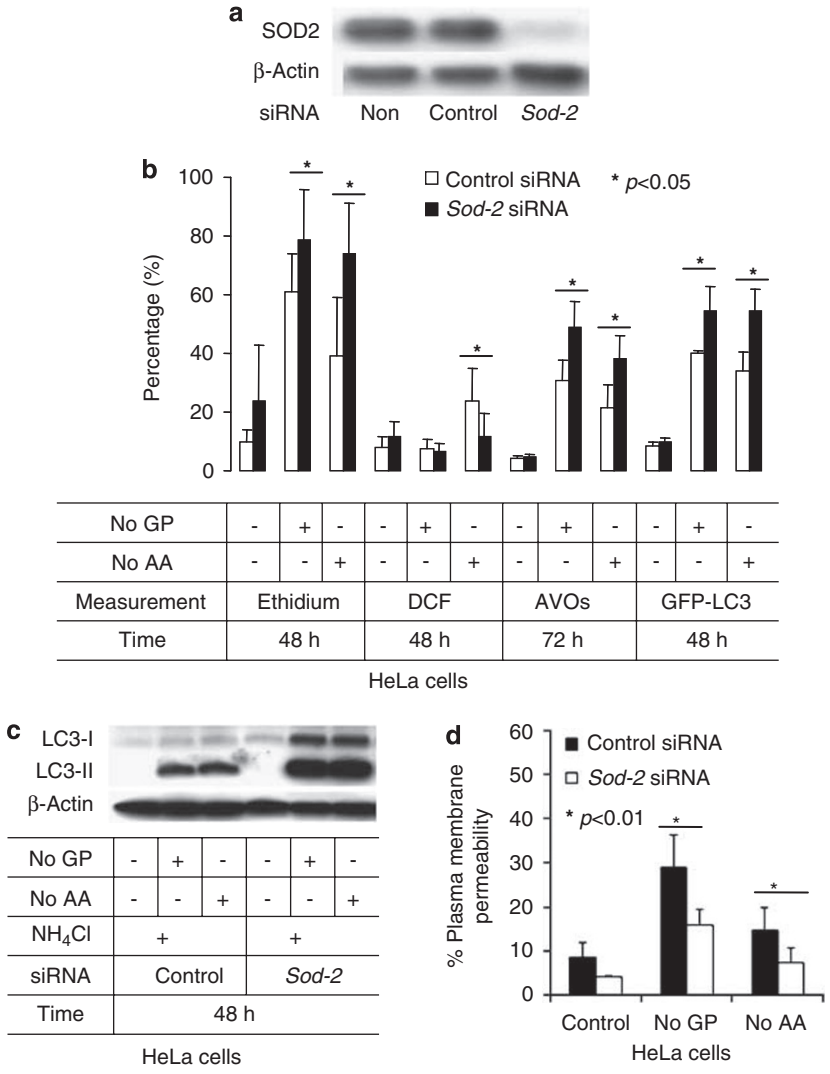

Figure 4 siRNA knockdown of *sod-2* upregulates autophagy but downregulates cell death induced by GP or AA starvation in HeLa cells. (**a**) Western blot showing that SOD2 expression was reduced by *sod-2* siRNA. β-Actin was used as a loading control. (**b**) Effect of *sod-2* siRNA on ROS generation, formation of AVOs, and GFP-LC3 dots (puncta). The percentages of ethidium fluorescence and DCF fluorescence represent the levels of intracellular $O_2^{\bullet -}$ and H_2O_2, respectively, as described in Figure 1. (**c**) Effect of *sod-2* siRNA on formation of LC3-II. β-Actin was used as a loading control. Cells were treated with the lysosomal inhibitor NH_4Cl at 30 mM for the determination of autophagy flux. (**d**) Effect of *sod-2* siRNA on cell death. The percentage of plasma membrane permeability represents the percentage of cell death as described in Figure 2. Error bars represent standard deviation (S.D.). All data are representative of three independent experiments

starvation-induced autophagy. The percentage of cells with AVOs was decreased from 31 to 1% (GP starvation) or from 18 to 1% (AA starvation), and the percentage of cells with GFP-LC3 puncta was decreased from 40 to 11% (GP starvation) or from 38 to 11% (AA starvation) after catalase treatment (Figure 5a). Starvation-induced LC3-II protein level was also significantly reduced by catalase (Figure 5b). Cell death induced by GP and AA starvation was increased from 25 to 60% and from 13 to 39%, respectively, at 72 h of catalase treatment (Figure 5c). When another ROS scavenger, *N*-acetyl-cysteine (NAC) was used in HeLa cells, autophagy induced by GP or AA starvation was significantly reduced and cell death was increased (data not shown). Thus, catalase treatments lowered both $O_2^{\bullet -}$ and H_2O_2 levels and reduced starvation-induced autophagy but increased starvation-induced cell death.

Autophagy induced by mETC inhibitors is mediated by $O_2^{\bullet -}$. Besides starvation, many other stimuli are known to induce autophagy.[1,2] We sought to determine whether $O_2^{\bullet -}$ mediation of autophagy is specific to starvation conditions, or if it is regulating autophagy through other stimuli. Our previous studies indicate that mETC inhibitors (including complex I inhibitor rotenone, complex II inhibitor TTFA, and complex I/SOD inhibitor 2-ME[23,28]) can induce ROS-mediated autophagy and autophagic cell death in cancer cells.[17,18] In these studies, SOD2 overexpression reduced autophagy, supporting the involvement of $O_2^{\bullet -}$ in autophagy induction. However, by measuring ROS only with dihydroethidium (DHE), which is reported to detect $O_2^{\bullet -}$ specifically,[27] we failed to directly address the function of H_2O_2. Therefore, in the present study we investigated the relative functions of $O_2^{\bullet -}$ and H_2O_2 on autophagy induced by these

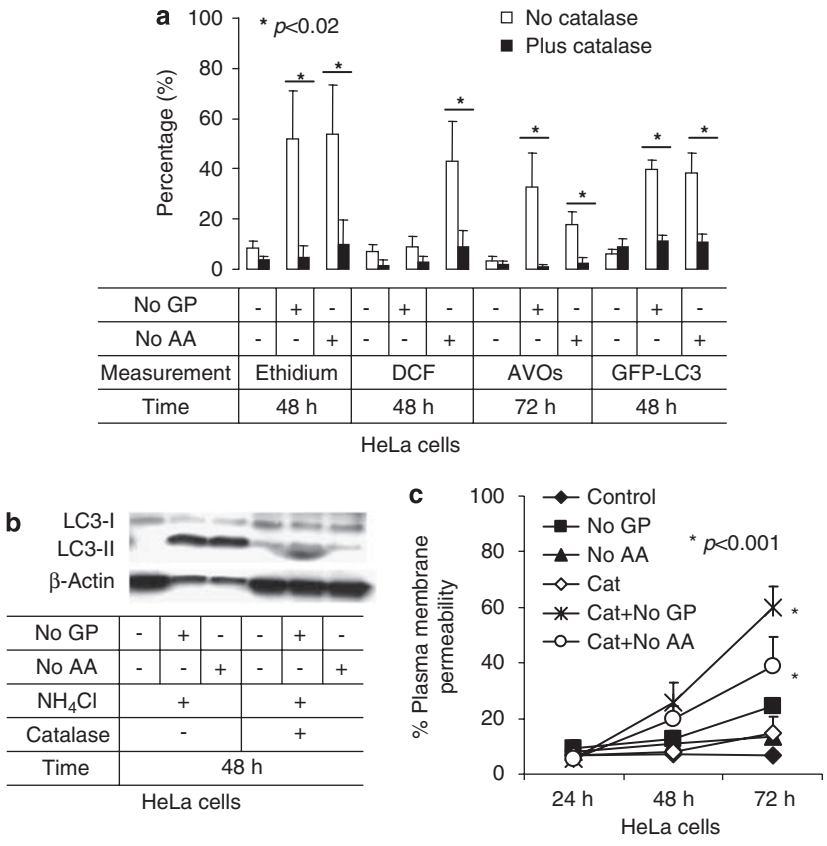

Figure 5 Catalase downregulates autophagy but upregulates cell death induced by GP or AA starvation in HeLa cells. (**a**) Effect of catalase (1000 U/ml) on ROS generation, formation of AVOs, and GFP-LC3 dots (puncta). The percentages of ethidium fluorescence and DCF fluorescence represent the levels of intracellular $O_2^{\bullet -}$ and H_2O_2, respectively, as described in Figure 1. (**b**) Effect of catalase (1000 U/ml) on formation of LC3-II at 48 h. β-Actin was used as a loading control. Cells were treated with the lysosomal inhibitor NH_4Cl at 30 mM for the determination of autophagy flux. (**c**) Effect of catalase (1000 U/ml) on cell death at 24, 48, and 72 h. The percentage of plasma membrane permeability represents the percentage of cell death as described in Figure 2. Error bars represent standard deviation (S.D.). All data are representative of three independent experiments

stimuli. Treatment with rotenone or TTFA causes increased production of $O_2^{\bullet -}$, which can be converted to H_2O_2 by SOD.[3,17] Because rotenone and TTFA can induce $O_2^{\bullet -}$ production at as early as 0.5 h, formation of GFP-LC3 puncta at 16 h, AVOs formation and cell death at 24 h,[17] we measured ROS at 6 and 24 h, formation of GFP-LC3 puncta and AVOs at 24 h, and cell death at 24 h, in the present study. When combined with 2-ME, the levels of $O_2^{\bullet -}$ induced by rotenone and TTFA were significantly increased from 46 to 57% and from 37 to 54%, respectively, in HeLa cells at 24 h (Figure 6a). Accordingly, 2-ME reduced the levels of H_2O_2 production from 59 to 38% following rotenone treatment and from 39 to 25% following TTFA treatment, in HeLa cells at 24 h (Figure 6a). Similar results were also obtained when HeLa cells were treated for 6 h (Supplementary Figure S6). In correlation with the increase in $O_2^{\bullet -}$ levels, the percentage of cells with GFP-LC3 puncta induced by rotenone and TTFA was also increased from 20 to 39% and from 22 to 34%, respectively, by the addition of 2-ME in HeLa cells at 24 h (Figure 6b). The protein level of LC3-II induced by rotenone or TTFA was also significantly increased with the addition of 2-ME (Figure 6c). Similar results were also obtained in HEK293 cells (Supplementary Figure S7). In HEK293 cells treated with rotenone or TTFA, the levels of $O_2^{\bullet -}$ production and autophagy (formation of green fluorescent protein (GFP) puncta and LC3-II) were both increased by the addition of 2-ME. Notably, H_2O_2 production was not significantly induced by rotenone, TTFA or 2-ME, alone or in combination (Supplementary Figure S7). Taken together, these data suggest that similar to starvation, autophagy induced by mETC inhibitors is regulated by $O_2^{\bullet -}$. In contrast to that starvation-induced autophagy reducing cell death, our previous study showed that rotenone-, TTFA-, or 2-ME-induced autophagy increases cell death.[17,18] In this study, cell death induced by the combination of rotenone and 2-ME or TTFA and 2-ME was also investigated. Figure 6d shows that cell death induced by rotenone and TTFA was increased from 20 to 30% and from 20 to 40%, respectively, following addition of addition of 2-ME. In contrast, 2-ME alone induced cell death of 13% compared to cell death of 8% in control at 24 h. Thus, different from that of starvation-induced autophagy, the enhancement of rotenone- or TTFA-induced autophagy (by 2-ME) leads to the enhancement of cell death.

Autophagy induced by exogenous H_2O_2 is mediated by $O_2^{\bullet -}$. Exogenous H_2O_2 is another stimulus known to induce autophagy.[7,9,12–16,21,29–31] In many previous *in vitro* studies,

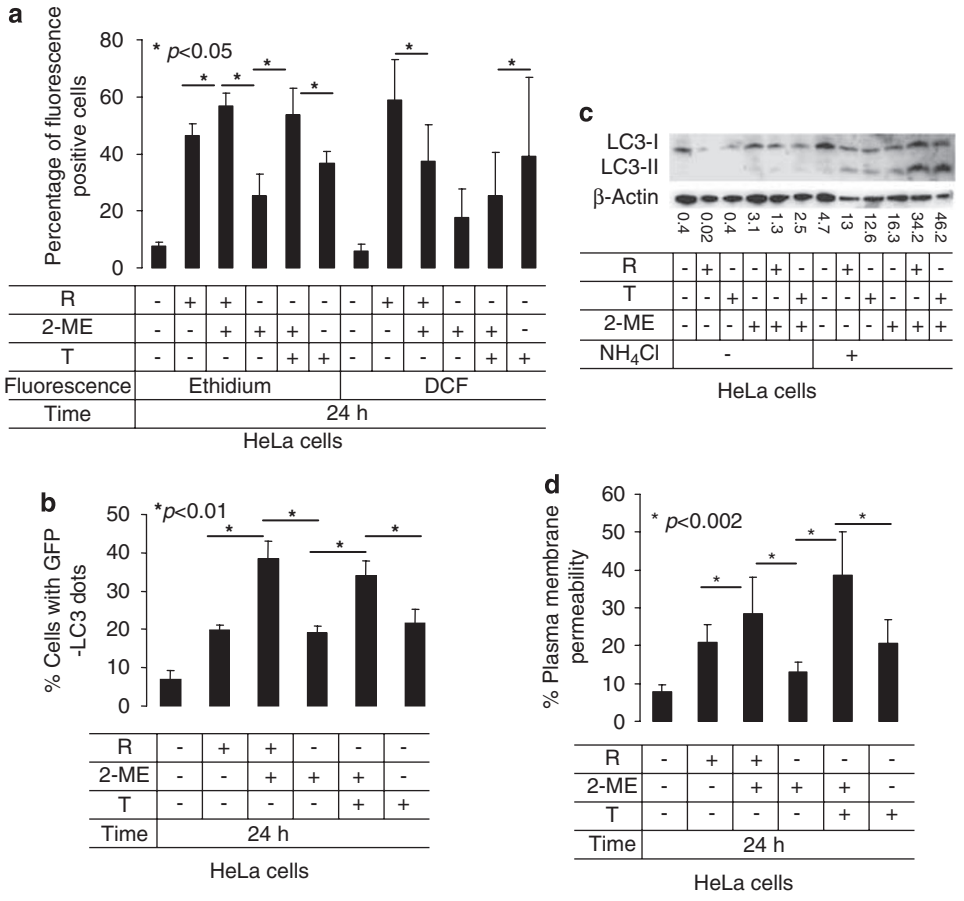

Figure 6 SOD inhibitor 2-ME upregulates autophagy and cell death induced by mETC inhibitors rotenone and TTFA in HeLa cells. Cells were treated with 0.1 mM 2-ME and/or 50 μM rotenone (R) and/or 0.5 mM TTFA (T) for 24 h. (**a**) ROS generation. The percentages of ethidium fluorescence and DCF fluorescence represent the levels of intracellular $O_2^{\bullet -}$ and H_2O_2, respectively, as described in Figure 1. (**b**) Formation of GFP-LC3 dots (puncta). (**c**) Formation of LC3-II. β-Actin was used as a loading control. Cells were treated with the lysosomal inhibitor NH_4Cl at 30 mM for the determination of autophagy flux. Numerical values indicate protein quantification by densitometry using QuantityOne software (Bio-Rad), normalized to β-actin. (**d**) Cell death. The percentage of plasma membrane permeability represents the percentage of cell death as described in Figure 2. Error bars represent standard deviation (S.D.). All data are representative of three independent experiments

addition of H_2O_2 has been used to mimic the effects of intracellularly produced H_2O_2, without actually measuring intracellular H_2O_2 because of the assumption that H_2O_2 can freely diffuse through biological membranes.[7,9,12–16,21,29–31] Indeed, our previous study showed that addition of exogenous H_2O_2 to HEK293, U87, and HeLa cells induced ROS production without directly measuring intracellular levels of H_2O_2.[18] In the current study, we investigated the functions of both intracellular $O_2^{\bullet -}$ and H_2O_2 on autophagy induced by exogenous H_2O_2. We found that the addition of exogenous H_2O_2 induced the production of intracellular $O_2^{\bullet -}$ but failed to increase intracellular H_2O_2 in HeLa cells (Figure 7a). Similar results were obtained in HEK293 cells: exogenous H_2O_2 induced $O_2^{\bullet -}$ production (Supplementary Figure S8a), formation of LC3-II (Supplementary Figure S8b) but failed to increase the production of intracellular H_2O_2 (Supplementary data Figure S8a). When SOD2 was overexpressed in HeLa cells (Figure 3a), $O_2^{\bullet -}$ production was greatly reduced from 77 to 10% whereas intracellular H_2O_2 production was significantly increased from 1 to 17% following treatment with exogenous H_2O_2 (Figure 7a). Along with decreasing intracellular $O_2^{\bullet -}$ levels, SOD2 overexpression significantly decreased the percentage of cells with AVOs from 21 to 4% (Figure 7a) and the LC3-II protein level (Figure 7b) following exogenous H_2O_2 treatment. These results implicate $O_2^{\bullet -}$ in regulating exogenous H_2O_2-induced autophagy.

Superoxide ($O_2^{\bullet -}$) production occurs upstream of PI3K class III and beclin-1 activation during starvation-induced autophagy. Scherz-Shouval *et al*.[15] showed that partial H_2O_2 was produced from downstream of PI3K class III-beclin-1 complex activation during AA starvation-induced autophagy.[15] In this study, we found that GP or AA starvation-induced H_2O_2 generation was increased by 3-MA (Figure 8a), whereas starvation-induced autophagy was decreased by 3-MA (Figure 2d; Supplementary Figure S4a), in HeLa cells. 3-MA treatment had no effect on $O_2^{\bullet -}$ levels in HeLa cells (Figure 8a). When another autophagy inhibitor wortmannin (Supplementary Figure S4bi) was used in HeLa cells, the levels of both $O_2^{\bullet -}$ and H_2O_2 induced by GP or AA starvation were not significantly affected (Figure 8b). In addition, *beclin-1* and *atg-7* siRNAs knockdown failed to significantly affect GP or AA starvation-

induced $O_2^{\bullet -}$ and H_2O_2 production in HeLa cells (Figure 8c). Thus, our results indicate that increased levels of $O_2^{\bullet -}$ following starvation occur upstream of PI3K class III-beclin-1 complex activation.

Discussion

Autophagy has been intensively studied in recent years. However, the mechanism of autophagy induction remains unclear. The involvement of ROS in autophagy has been

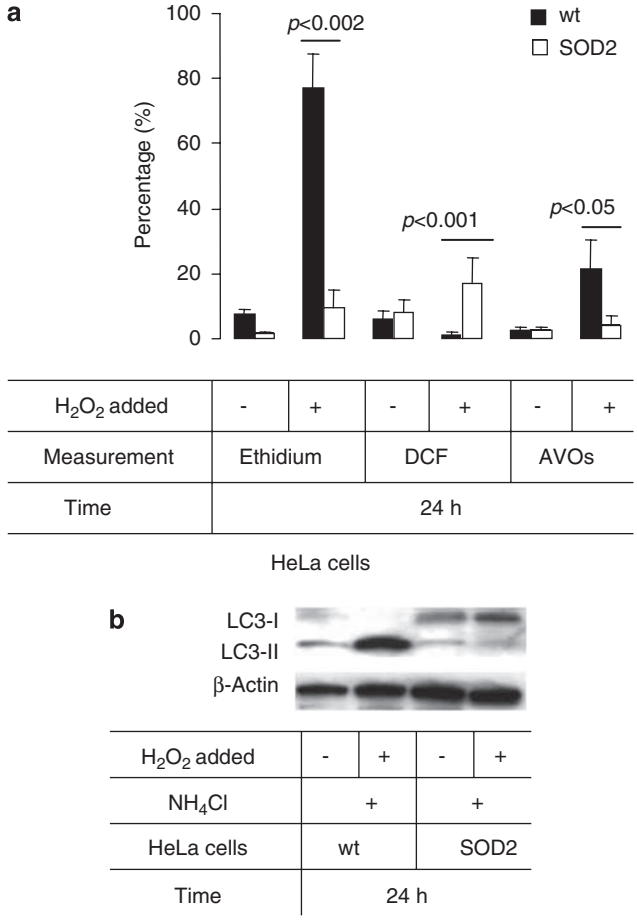

Figure 7 Overexpression of SOD2 downregulates autophagy induced by exogenous H_2O_2 in HeLa cells. Cells were treated with 1 mM H_2O_2 for 24 h. (**a**) Effect of SOD2 overexpression on ROS generation and AVOs formation. The percentages of ethidium fluorescence and DCF fluorescence represent the levels of intracellular $O_2^{\bullet -}$ and H_2O_2, respectively, as described previously. (**b**) Effect of SOD2 overexpression on LC3-II formation. β-Actin was used as a loading control. Cells were treated with the lysosomal inhibitor NH_4Cl at 30 mM for the determination of autophagy flux. Error bars represent standard deviation (S.D.). All data are representative of three independent experiments

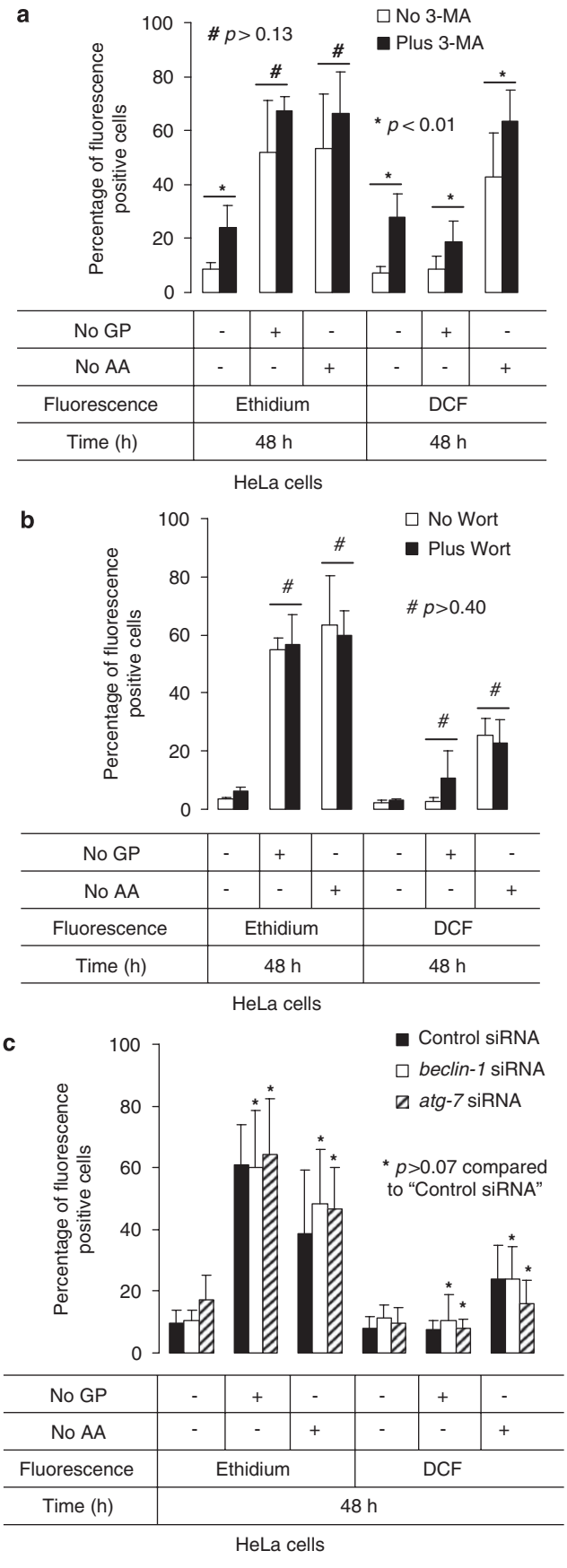

Figure 8 Effects of autophagy inhibitors on ROS generation induced by GP or AA starvation in HeLa cells. (**a**) Effect of 3-MA (2 mM) at 48 h. (**b**) Effect of wortmannin (Wort, 0.2 μM) at 48 h. (**c**) Effect of *beclin-1* and *atg-7* siRNAs at 48 h. The percentages of ethidium fluorescence and DCF fluorescence represent the levels of intracellular $O_2^{\bullet -}$ and H_2O_2, respectively, as described in Figure 1. Error bars represent standard deviation (S.D.) from three independent experiments

demonstrated in many studies,[5–22] but the relative functions of $O_2^{\bullet-}$ and H_2O_2 are not well established. In this study, we have compared the relative functions of $O_2^{\bullet-}$ and H_2O_2 in the regulation of autophagy induced by AA and GP starvation conditions, mETC inhibitors, and exogenous H_2O_2. Our findings indicate for the first time that autophagy is selectively mediated by $O_2^{\bullet-}$, and that exogenous H_2O_2 is effectively converted to intracellular $O_2^{\bullet-}$ leading to induction of autophagy.

Reactive oxygen species are regulated by a series of antioxidant enzymes. Because SOD is the antioxidant enzyme to convert $O_2^{\bullet-}$ to H_2O_2,[2,3] the level of $O_2^{\bullet-}$ can be controlled by modulating SOD activity. The findings from this study indicate that upregulation of autophagy can be achieved by inhibiting SOD to elevate $O_2^{\bullet-}$ levels, and that activating SOD can downregulate autophagy. Activation of downstream antioxidant enzymes that catalyze H_2O_2 to H_2O such as catalase, GPx, and PrxIII can also reduce autophagy levels.[2] However by reducing H_2O_2 level, the levels of $O_2^{\bullet-}$ are also reduced through a chain reaction.[2,3] This illustrates the importance for measuring all forms of ROS.

One interesting phenomenon observed from this study is that two different starvation conditions (GP and AA starvation) induce different spectra of ROS production in a same type of cells. GP starvation induces $O_2^{\bullet-}$ production but not H_2O_2, whereas AA starvation induces both $O_2^{\bullet-}$ and H_2O_2 production. Because both starvation conditions induce autophagy, it should be expected that $O_2^{\bullet-}$ is the ROS-mediating autophagy. However, the AA starvation system is widely used for autophagy studies, and both $O_2^{\bullet-}$ and H_2O_2 are simultaneously produced in this type of starvation.[15] There are several possible reasons why H_2O_2 is the more commonly investigated ROS, whereas the function of $O_2^{\bullet-}$ has been neglected under AA starvation. First, because $O_2^{\bullet-}$ and H_2O_2 are simultaneously produced under AA starvation, they could have redundant function in autophagy regulation. Second, H_2O_2 is more stable than $O_2^{\bullet-}$ and is found to be a signaling molecule in many biological pathways. Third, H_2O_2 scavengers such as catalase and NAC are readily available.[3] Fourth, many studies use exogenous H_2O_2 as a control to mimic the effect of intracellularly produced H_2O_2. We show, however, that it is not possible to specify whether $O_2^{\bullet-}$ or H_2O_2 is the mediator of AA starvation-induced autophagy simply based on the effect of H_2O_2 scavengers or the addition of exogenous H_2O_2. H_2O_2 scavengers such as catalase and NAC also effectively scavenge $O_2^{\bullet-}$ because $O_2^{\bullet-}$ can be quickly converted to H_2O_2 by SOD in the cell, and exogenous H_2O_2 can effect on the cells to produce $O_2^{\bullet-}$ possibly by damaging mETC.

One interesting question is the source of ROS induced by starvation. Scherz-Shouval *et al*.[15] demonstrated that significant amount of AA starvation-induced H_2O_2 is located in mitochondria. Our results showed that overexpression or knockdown (by siRNA) of the mitochondria-localized SOD2 decreased or increased starvation-induced $O_2^{\bullet-}$ also indirectly indicate that mitochondria are an important source of starvation-induced ROS. The localization of starvation-induced ROS will be the focus for future studies.

Some discrepancies exist on the time of ROS production and autophagy induced by AA starvation between this study and other studies from the literature. For example, several groups have shown that ROS and autophagy can be detected at earlier times (between 2 and 4 h) whereas this study showed that ROS and autophagy can only be detected after 6 h. This could be due to the variations of cell lines used, the relative health of the cells before starvation, and/or differences in detailed experimental procedures from different laboratories. Because earlier studies did not quantify both ROS species, $O_2^{\bullet-}$ and H_2O_2, simultaneously, but emphasized on H_2O_2 quantification, it is quite possible that these difference could also be due to the type of ROS detected. Nevertheless, the correlation between ROS production and induction of autophagy remains consistent in these studies.

Starvation-induced autophagy is associated with cell survival whereas autophagy induced by various other stimuli (including dopamine,[8] sodium selenite,[13] mETC inhibitors rotenone and TFFA,[17] SOD2 inhibitor 2-ME,[18] and exogenous H_2O_2[12,18]) is associated with cell death. We and others have found that these inducers of autophagy require ROS production.[8,13,12,18] Indeed, we have previously found that rotenone and TTFA induce $O_2^{\bullet-}$ production and that overexpressing SOD2 blocks autophagy.[17] This was reversed by knocking down SOD2 by siRNA. The data in the current study showed that combining the SOD2 inhibitor 2-ME with an mETC inhibitor increased $O_2^{\bullet-}$ production, autophagy, and cell death. 2-ME is currently in clinical trials for treating cancers and might potentiate cell death through increased $O_2^{\bullet-}$ production and induction of autophagy. Alternatively, increasing $O_2^{\bullet-}$ production by using *sod-2* siRNA could lead to cell survival under starvation conditions. In contrast, decreasing $O_2^{\bullet-}$ production by SOD2 overexpression, catalase, or NAC reduced autophagy but increased cell death under starvation conditions. Therefore, autophagy can lead to cell survival and cell death under different stimuli even in a same type of cells. The complete mechanisms regulating autophagy-induced cell survival and cell death remain to be determined.

Exogenous H_2O_2 is frequently used to mimic the effect of intracellularly produced H_2O_2 and has been shown to induce autophagy.[7,9,12–16,21] However, in these studies, the intracellular levels of $O_2^{\bullet-}$ and H_2O_2 induced by exogenous H_2O_2 were not directly measured. We found that exogenous H_2O_2 increases the generation of intracellular $O_2^{\bullet-}$ but failed to change levels of intracellular H_2O_2 (Figure 7; Supplementary Figure S8). These findings indicate that exogenous H_2O_2 induces autophagy through the generation of intracellular $O_2^{\bullet-}$ (Figure 7; Supplementary Figure S8; Chen *et al*.[18]). This emphasizes the importance for determining the relative levels of $O_2^{\bullet-}$ and H_2O_2.

Reactive oxygen species induces multiple downstream signals. We showed that $O_2^{\bullet-}$ production occurs upstream of the activation of beclin-1 and PI3K class III and leads to induction of autophagy. In contrast, others have shown that blockage of PI3K class III activation with 3-MA or wortmannin prevents H_2O_2 production following AA starvation.[15] This could be due to cell-type-specific differences or the lack of determination of the relative amounts of $O_2^{\bullet-}$ and H_2O_2 produced by AA starvation. Nevertheless, ROS could act further downstream by oxidizing Atg-4 and/or increasing beclin-1 expression leading to induction of autophagy.[15,18]

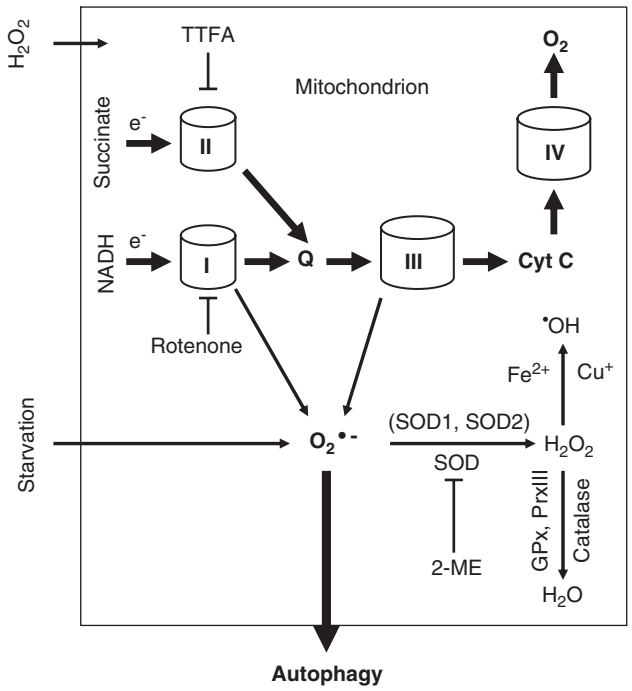

Figure 9 Model of autophagy induction mediated by superoxide ($O_2^{\bullet-}$). Autophagy can be induced by various stimuli such as starvation, mETC inhibitors rotenone and TTFA, the SOD inhibitor 2-ME, and exogenous H_2O_2. I, II, III, and IV represent mETC complexes I, II, III, and IV, respectively. 2-ME, 2-methoxyestradiol; Cyt C, cytochrome *c*; Q, ubiquinone–ubiquinol pool; GPx, glutathione peroxidase; PrxIII, peroxiredoxin III; SOD, superoxide dismutase; SOD1, Cu, Zn-SOD; SOD2, Mn-SOD. Arrows represent activation. Bars represent inhibition. Catalase can be found in cytoplasm and mitochondria[33]

However, exact downstream signaling events regulated by $O_2^{\bullet-}$ leading to autophagy are unknown and will be the focus for future investigations.

Although we cannot exclude the possibility that H_2O_2 may be involved in autophagy regulation in other types of cells and with other stimuli, we propose a model for autophagy induction mediated by $O_2^{\bullet-}$ as shown in Figure 9. In our model, starvation, addition of exogenous H_2O_2, inhibition of SOD, or blockade of the electron transport chain causes increased $O_2^{\bullet-}$ leading to autophagy. Because autophagy is involved in many human pathologies,[32] our studies of autophagy regulation could provide insights for the development of novel drugs or approaches for controlling autophagy through $O_2^{\bullet-}$ regulation in human diseases.

Materials and Methods

Reagents. Acridine orange, 3-MA, wortmannin, H_2O_2, 2-ME, rotenone, TTFA, DAPI (4′,6-diamidino-2-phenylindole), catalase, and medium for GP (glucose, L-glutamine, sodium pyruvate, phenol red, $NaHCO_3$, and serum) starvation were purchased from Sigma-Aldrich (Oakville, Ontario, Canada). Medium for AA (amino acids and serum) starvation (EBSS) was purchased from HyClone Laboratories Inc. (Logan, UT, USA). Dihydroethidium (DHE) and 5-(and-6)-chloromethyl-2′, 7′-dichlorodihydrofluorescein diacetate acetyl ester (CM-H2DCFDA) were from Invitrogen (Burlington, Ontario, Canada). DHE, 2-ME, rotenone, TTFA, and DAPI were dissolved in dimethyl sulfoxide (DMSO). Catalase, 3-MA, and H_2O_2 were dissolved in double-distilled water. The final concentration of DMSO in media was less than 0.1% and it did not have any effect on the activities tested in this study (data of DMSO effect are not shown in this study). The concentrations of reagents used in this study were: H_2O_2, 1.0 mM; 2-ME, 0.1 mM; 3-MA, 2.0 mM; wortmannin, 0.2 μM; DHE, 3.2 μM; CM-H2DCFDA, 5 μM; rotenone, 50 μM; TTFA, 0.5 mM; and DAPI, 3.0 μM.

Antibodies and siRNAs. Beclin-1 primary antibody and its secondary antibody donkey anti-goat HRP were purchased from Santa Cruz Biotechnology Inc. (Santa Cruz, CA, USA). ATG-7 antibody was purchased from PromoKine Inc. (Germany). SOD2 antibody was purchased from StressGen Biotechnologies (Victoria, Canada). Rabbit anti-actin antibody was purchased from Sigma, rabbit anti-LC3 antibody from Abgent Inc. and their secondary antibody goat anti-rabbit IgG(H + L) HRP from Bio-Rad Laboratories. anti-LC3 mouse monoclonal antibody was purchased from NanoTools and its goat anti-mouse IgG(H + L) HRP from Bio-Rad Laboratories. The siRNAs specific for human *beclin-1*, *atg-7*, and *sod-2* are same as in our previous study.[18]

Cell culture. Human embryonic kidney cell line HEK293, human glioma cancer cell line U87, and human cervical cancer cell line HeLa were maintained in a humidified 5% CO_2, 37°C incubator in Dulbecco's modified Eagle's medium supplemented with 100 U/ml penicillin, 100 μg/ml streptomycin (Invitrogen). Media used for HEK293 and HeLa were supplemented with 10% bovine calf serum and 10% fetal bovine serum (FBS) (Invitrogen), respectively. Medium for the stabilized HeLa cells with overexpression of SOD2 was also supplemented with 0.2 mg/ml G418 (Life Technologies Inc.). Medium for U87 was supplemented with 10% FBS, 1 mM sodium pyruvate, and 2 mM glutamine without penicillin and streptomycin.

Silencing *beclin-1*, *atg-7*, or *sod-2* genes by siRNA. The methods for transfection of siRNA into cells and for the treatment of cells have been described in our previous studies.[17,18]

Flow cytometric quantification of AVOs. The method is same as described in our previous studies.[17,18]

Staining autophagosomes with GFP-LC3. The method is same as described in our previous studies.[17,18] Cells transfected with GFP alone plasmid did not show punctate green dots (vacuoles) when treated with starvation, mETC inhibitors, 2-ME or H_2O_2, and therefore the results have not been demonstrated in this study. Only the results of cells transfected with GFP-LC3 plasmid have been demonstrated.

Flow cytometric analysis of ROS. Reactive oxygen species generation was determined by flow cytometry after cells were stained with DHE or CM-H2DCFDA . DHE and CM-H2DCFDA are used to specifically detect the generation of intracellular $O_2^{\bullet-}$ and H_2O_2, respectively.[27] DHE is oxidized to red fluorescent ethidium by $O_2^{\bullet-}$[17,18,27] and CM-H2DCFDA is oxidized to green fluorescent DCF (dichlorofluorescein) by H_2O_2.[27] For staining of cells, cells were centrifuged and the pellet was resuspended in 0.2 ml PBS in an Eppendorf tube. DHE with a final concentration of 3.2 μM or CM-H2DCFDA with a final concentration of 5 μM was added into the cell suspension and was gently mixed. The mixture was incubated in dark in a water bath at 37°C for 15 min. Then, the cell suspension was transferred into a 5 ml FALCON FACS tube and analyzed on a flow cytometer using CellQuest software (Becton Dickinson, San Jose, CA, USA) within 10 min. Alternatively, cells can be stained with DHE or CM-H2DCFDA for 15 min before trypsinization (for attachment cells). Actually, these two cell staining methods gave similar results (Supplementary data Figure S1). In this study, ROS have been measured by staining cells with DHE or CM-H2DCFDA after trypsinizing cells, removing trypsin, and resuspending cells in PBS.

Flow cytometric analysis of cell death. Cell death was detected by measuring the plasma membrane permeability to Trypan blue as described previously.[18] Briefly, cell pellet was collected and resuspended in 200 μl PBS in an FACS tube. Then, Trypan blue with a final concentration of 0.04% was added into the cell suspension. Then cells were stained for 5 min at room temperature and analyzed on a flow cytometer using CellQuest software (Becton Dickinson). Histogram data on log scale were collected on the red filter (675 nm, FL3-H). Two peaks in a histograph could be observed. The first peak represents viable cells, which were dimly fluorescent and not permeable to Trypan blue. The second peak represents dead cells, which were brightly fluorescent and permeable to Trypan blue. Results were confirmed by staining cells with AO and ethidium bromide and counting cells under a fluorescent microscope as described previously.[17,18]

Western blot analysis. Western blot analysis was performed as stated previously.[17,18] Tris-glycine SDS-PAGE was used, except for the detection of conversion of LC3-I (18 kDa, cytoplasmic form) to CL3-II (16 kDa, preautophagosomal and autophagosomal membrane-bound form), where Tris-Tricine SDS-PAGE was used. To determine autophagy flux, we used the lysosomal inhibitor NH_4Cl at 30 mM to treat cells before LC3-II western blot was performed. Densitometry was performed using QuantityOne software (Bio-Rad).

Statistical analysis. All experiments were repeated at least three times and each experiment was carried out at least by duplicates. The data were expressed as means ± S.D. (standard deviation) ($n \geqslant 3$). Statistical analysis was performed by using Student's *t*-test employing at least three independent data points. The criterion for statistical significance was $P < 0.05$. The software used was Excel or Sigma blot.

Acknowledgements. The work was supported by a grant from CancerCare Manitoba Foundation. YC was supported by a post-doctoral fellowship from Manitoba Health Research Council (MHRC). MBA was supported by a US Army Department of Defense Breast Cancer Research Program Predoctoral Traineeship Award. SBG is a Manitoba Research Chair supported by MHRC.

1. Levine B, Yuan J. Autophagy in cell death: an innocent convict? *J Clin Invest* 2005; **115**: 2679–2688.
2. Azad MB, Chen Y, Gibson SB. Regulation of autophagy by reactive oxygen species (ROS): implications for cancer progression and treatment. *Antioxid Redox Signal* 2008; **11**: 777–790.
3. Chen Y, Gibson SB. Is mitochondrial generation of reactive oxygen species a trigger for autophagy? *Autophagy* 2008; **4**: 246–248.
4. Ozben T. Oxidative stress and apoptosis: impact on cancer therapy. *J Pharm Sci* 2007; **96**: 2181–2196.
5. Bridges KR. Ascorbic acid inhibits lysosomal autophagy of ferritin. *J Biol Chem* 1987; **262**: 14773–14778.
6. Lemasters JJ, Nieminen AL, Qian T, Trost LC, Elmore SP, Nishimura Y *et al.* The mitochondrial permeability transition in cell death: a common mechanism in necrosis, apoptosis and autophagy. *Biochim Biophys Acta* 1998; **1366**: 177–196.
7. Kirkland RA, Adibhatla RM, Hatcher JF, Franklin JL. Loss of cardiolipin and mitochondria during programmed neuronal death: evidence of a role for lipid peroxidation and autophagy. *Neuroscience* 2002; **115**: 587–602.
8. Gómez-Santos C, Ferrer I, Santidrián AF, Barrachina M, Gil J, Ambrosio S. Dopamine induces autophagic cell death and alpha-synuclein increase in human neuroblastoma SH-SY5Y cells. *J Neurosci Res* 2003; **73**: 341–350.
9. Djavaheri-Mergny M, Amelotti M, Mathieu J, Besançon F, Bauvy C, Souquère S *et al.* NF-κB activation represses tumor necrosis factor-α-induced autophagy. *J Biol Chem* 2006; **281**: 30373–30382.
10. Kiffin R, Bandyopadhyay U, Cuervo AM. Oxidative stress and autophagy. *Antioxid Redox Signal* 2006; **8**: 152–162.
11. Kissová I, Deffieu M, Samokhvalov V, Velours G, Bessoule JJ, Manon S *et al.* Lipid oxidation and autophagy in yeast. *Free Radic Biol Med* 2006; **41**: 1655–1661.
12. Byun YJ, Lee SB, Kim DJ, Lee HO, Son MJ, Yang CW *et al.* Protective effects of vacuolar H+-ATPase c on hydrogen peroxide-induced cell death in C6 glioma cells. *Neurosci Lett* 2007; **425**: 183–187.
13. Kim EH, Sohn S, Kwon HJ, Kim SU, Kim MJ, Lee SJ *et al.* Sodium selenite induces superoxide-mediated mitochondrial damage and subsequent autophagic cell death in malignant glioma cells. *Cancer Res* 2007; **67**: 6314–6324.
14. Kunchithapautham K, Rohrer B. Apoptosis and autophagy in photoreceptors exposed to oxidative stress. *Autophagy* 2007; **3**: 433–441.
15. Scherz-Shouval R, Shvets E, Fass E, Shorer H, Gil L, Elazar Z. Reactive oxygen species are essential for autophagy and specifically regulate the activity of Atg4. *EMBO J* 2007; **26**: 1749–1760.
16. Xiong Y, Contento AL, Nguyen PQ, Bassham DC. Degradation of oxidized proteins by autophagy during oxidative stress in Arabidopsis. *Plant Physiol* 2007; **143**: 291–299.
17. Chen Y, McMillan-Ward E, Kong J, Israels SJ, Gibson SB. Mitochondrial electron-transport-chain inhibitors of complexes I and II induce autophagic cell death mediated by reactive oxygen species. *J Cell Sci* 2007; **120**: 4155–4166.
18. Chen Y, McMillan-Ward E, Kong J, Israels SJ, Gibson SB. Oxidative stress induces autophagic cell death independent of apoptosis in transformed and cancer cells. *Cell Death Differ* 2008; **15**: 171–182.
19. Chen F, Wang CC, Kim E, Harrison LE. Hyperthermia in combination with oxidative stress induces autophagic cell death in HT-29 colon cancer cells. *Cell Biol Int* 2008; **32**: 715–723.
20. Dadakhujaev S, Noh HS, Jung EJ, Hah YS, Kim CJ, Kim DR. The reduced catalase expression in TrkA-induced cells leads to autophagic cell death via ROS accumulation. *Exp Cell Res* 2008; **314**: 3094–3106.
21. Pyo JO, Nah J, Kim HJ, Lee HJ, Heo J, Lee H *et al.* Compensatory activation of ERK1/2 in Atg5-deficient mouse embryo fibroblasts suppresses oxidative stress-induced cell death. *Autophagy* 2008; **4**: 315–321.
22. Yang J, Wu LJ, Tashino S, Onodera S, Ikejima T. Reactive oxygen species and nitric oxide regulate mitochondria-dependent apoptosis and autophagy in evodiamine-treated human cervix carcinoma HeLa cells. *Free Radic Res* 2008; **42**: 492–504.
23. Huang P, Feng L, Oldham EA, Keating MJ, Plunkett W. Superoxide dismutase as a target for the selective killing of cancer cells. *Nature* 2000; **407**: 390–395.
24. Azad MB, Chen Y, Henson ES, Cizeau J, McMillan-Ward E, Israels SJ *et al.* Hypoxia induces autophagic cell death in apoptosis-competent cells through a mechanism involving BNIP3. *Autophagy* 2008; **4**: 195–204.
25. Mizushima N, Yoshimori T. How to interpret LC3 immunoblotting. *Autophagy* 2007; **3**: 542–545.
26. Klionsky DJ, Abeliovich H, Agostinis P, Agrawal DK, Aliev G, Askew DS *et al.* Guidelines for the use and interpretation of assays for monitoring autophagy in higher eukaryotes. *Autophagy* 2008; **4**: 151–175.
27. Gao N, Rahmani M, Dent P, Grant S. 2-Methoxyestradiol-induced apoptosis in human leukemia cells proceeds through a reactive oxygen species and Akt-dependent process. *Oncogene* 2005; **24**: 3797–3809.
28. Hagen T, D'Amico G, Quintero M, Palacios-Callender M, Hollis V, Lam F *et al.* Inhibition of mitochondrial respiration by the anticancer agent 2-methoxyestradiol. *Biochem Biophys Res Commun* 2004; **322**: 923–929.
29. Kulisz A, Chen N, Chandel NS, Shao Z, Schumacker PT. Mitochondrial ROS initiate phosphorylation of p38 MAP kinase during hypoxia in cardiomyocytes. *Am J Physiol Lung Cell Mol Physiol* 2002; **282**: L1324–L1329.
30. Nonn L, Berggren M, Powis G. Increased expression of mitochondrial peroxiredoxin-3 (thioredoxin peroxidase-2) protects cancer cells against hypoxia and drug-induced hydrogen peroxide-dependent apoptosis. *Mol Cancer Res* 2003; **1**: 682–689.
31. Li J, Li Q, Xie C, Zhou H, Wang Y, Zhang N *et al.* Beta-actin is required for mitochondria clustering and ROS generation in TNF-induced, caspase-independent cell death. *J Cell Sci* 2004; **117**: 4673–4680.
32. Mizushima N, Levine B, Cuervo AM, Klionsky DJ. Autophagy fights disease through cellular self-digestion. *Nature* 2008; **451**: 1069–1075.
33. Radi R, Turrens JF, Chang LY, Bush KM, Crapo JD, Freeman BA. Detection of catalase in rat heart mitochondria. *J Biol Chem* 1991; **266**: 22028–22034.

Supplementary Information accompanies the paper on Cell Death and Differentiation website (http://www.nature.com/cdd)